CHAPTER IV

EXPERIMENTAL RESULTS

The experiments were made under the operating conditions summarized in Table 3.1. Typical experimental data and results are tabulated in Appendix A. The results were divided into 3 parts.

4.1 Part A: Malaysian Size

Chips mechanically cut by Malaysian machines were tested and compared with those tested by Thanh[1] who studied them by using sun-drying method. The Malaysian cutter produced tapioca slices 0.2-0.3 cm. thick.

Slices produced by this Malaysian cutter were dried under various conditions. The variables used were air flowrate, bed depth and hot air temperature. The results are shown in Table 4.1 and Figure 4.1 to Figure 4.5. Table. 4.1 shows the summary of the results of part A: that is the influence of air flow rate, air temperature and bed loading on the drying time. The drying time was reduced remarkably as hot air temperature and air flow rate were raised; and when the bed loading was small.

Figure 4.1 shows the plots of water content with the time in dryer for run no. A-1, A-2, A-3 and A-4 at four different air flow rates i.e., 762, 1,144, 1,524 and 2,096 Kg/hr.m^2 respectively. The plots showed that air flow rate had an important effect on the drying. It is noted that the time required for run no. A-1 was approximately double to that of run no.A-4 for the chips to reach water content of 0.1 Kg Water/Kg dry solid.

Figures 4.2 and 4.3 show similar plots to Figure 4.1 but at different hot air temperature and bed loading respectively. They showed clearly the influence of both variables on the drying. Especially, when the temperature was the variable, it showed much influence on the drying. In contrast between run no. A-3 (80°C) and run no. A-7 (40°C), the drying times for the water content to reach 0.1 Kg Water/Kg dry solid were very different. In run no. A-3 the time was 124 min. while in run no.A-7 the time was 340 min, the difference was more than 3 hours. This was due to the increase in heat transfer by conduction and in mass transfer by diffusion in the tapioca chips as the temperature was increased.

Figure 4.4 shows the plots of rate of drying for run no. A-3 (80°C), A-7 (60°C) and A-8 (40°C) with water content. The plots showed that the run with higher hot air temperature would have the greater drying rate. All drying-rate curves decreased gradually along with the decreasing water content.

Figure 4.5 shows the comparison between the results from the through-circulation drying and those from sun-drying method made on concrete and black concrete surface.(1)

Run no. S_1, S_2 in Fig. 4.5 were carried out during the hot season, between March and July 1975, when the air temperature varied between 28 and 35°C. The record of the data was started at 8 A.M.

In run no. S_1 and S_2, 14 percent water content was attained in 0.2 - 0.3 cm. slices after about 8 and 10 hours of drying respectively. For through-circulation drying, the time to reach the same water content was only 1 to 2 hours.

4.2 Part B: Definite Size

4.2.1 Variable: Air flow rate

Six runs were carried out. In these runs the air flow rate was varied from 1,144 Kg/hr.m^2 to 2,096 Kg/hr.m^2 while other controllable parameters, i.e., hot air temperature, chip size and bed loading were held constant. For the first three runs the constant bed loading used was 32.1 Kg.B.D.S./m^2 and the second three runs, it was 10 Kg.B.D.S./m^2. The air temperature was 80°C and chip size was 2x6x0.5 cm. The results are shown graphically in Figure 4.6 to Figure 4.9. The plots showed clearly that the water content decreased remarkably as air flow rate was raised. For example as shown in Fig. 4.6 to reduce the water

content from 1.531 Kg water/Kg.dry solid to 0.2 Kg.water/Kg.dry solid, drying time required would be about 200, 174 and 136 minutes for air flow rate of 1,144, 1,524 and 2,096 Kg/hr.m^2 respectively. Drying rates, in Kg. of water evaporated per Kg. of dry solid per minute per square meter were calculated and plotted versus average water content. The results of run No. B-1, B-2 and B-3 are shown in Figure 4.7. It can be noted that hot air flow rate had strong influence on the drying rate. The drying rate was highly increased as the air flow rate was raised from 1,144 (B-3) to 2,096 (B-1) Kg/hr.m^2.

Figure 4.8 and Figure 4.9 show similar plots to Figure 4.6 and 4.7 for run no. B-4, B-5 and B-6 at bed loading of 22.3 Kg.B.D.S./m^2.

4.2.2 Variable: Bed loading

Two series of runs were carried out. In this experiment the bed loadings were varied from 9.1 Kg. B.D.S./m^2 to 38.7 Kg.B.D.S./m^2 (or bed depth about 5 cm. to 20 cm). Other variables, i.e., hot air temperature, chip size and air flow rate were kept constant at 80°C, 2x6x0.3 cm. and 1,524 Kg/hr.m^2 for first series (run no. B-7 to B-10) or 2,096 Kg/hr.m^2 for second series (run no. B-11 to B-13) respectively. The results are shown graphically in Figure 4.10 to Figure 4.13. The curves showed the pronounced effect of the bed loading on the drying of tapioca. The water content decreased faster as the

bed loading was decreased. For example as shown in Figure 4.10 to reduce the water content from 1.462 Kg water/Kg dry solid to 0.1 Kg water/Kg dry solid, drying times in dryer were 224, 160, 136 and 102 minutes for bed loadings of 38.7, 24.5, 18.4 and 9.1 Kg B.D.S./m^2 respectively. In Figure 4.11 drying rates were plotted against water content. It is noted that bed loading also played an important role in drying of the tapioca chips. the more bed loading used, the slower rate of drying was.

Figure 4.12 and 4.13 show similar plots to Figure 4.10 and 4.11 for run no. B-11 to B-13 at air flow rate of 2,096 Kg/hr.m^2. Bed loading still had effect on the drying rates but not so pronounced as the previous results.

4.2.3 Variable: Hot air temperature

The results are presented graphically in Figure 4.14 to 4.17. Two series of runs were made. Hot air temperature was varied from 60°C to 90°C. Other variables, i.e., air flow rate, chip size and bed loading were fixed. In the first series (run no. B-14 to B-17) air flow rate was fixed at 2,096 Kg/hr.m^2 and bed loading at 32.1 Kg.B.D.S./m^2. In the second series (run no. B-18 to B-20) air flow rate was held constant at 1,524 Kg/hr.m^2. and bed loading at 18.4 Kg B.D.S./m^2. (chip size of the first series was 2x6x0.5 cm. and that of the second series was 2x6x0.3 cm.)

The curves in Figure 4.14 shows that the water content was decreased remarkably as hot air temperature was raised. For example, to reduce the water content from 1.531 Kg.water/Kg. dry solid to 0.1 Kg.water/Kg dry solid., drying time required would be about 276, 204, 180 and 154 minutes for drying temperature of 60°(B-17), 70°(B-16), 80°(B-15), and 90°C (B-14) respectively. The drying times of run no. B-17 differed so much from those of the other three runs.

Figure 4.15 shows the strong influence of the air temperature on the drying rate of tapioca.

Figure 4.16 and 4.19 also show the influence of the hot air temperature on the drying in the same manner as just mentioned.

4.2.4 Variable: Chip thickness

The results are presented graphically in Figure 4.18 to 4.21. Two series of runs were made. In the first series (run no. B-21 to B-23) bed depth was fixed at 10 cm. and the second series (run no. B-24 to B-26) bed depth was fixed at 15 cm. The bed loadings were different for different chip sizes. The thickness of the chip was varied from 0.3 to 0.7 cm. Hot air temperature was fixed at 80°C and air flow rates at 1,524 Kg/hr.m^2. Figure 4.18 and 4.19 show the influence of the thickness on the drying. The drying time of the thin chips was less than that of the thicker ones. For example in Figure 4.18, to reduce the water content from 1.507 Kg water/Kg dry solid to 0.15 Kg water/Kg dry solid, drying times required were 192, 152 and 118 minutes

for chip thickness of 0.7 (B-23), 0.5 (B-22) and 0.3 (B-21) cm. respectively. Figure 4.20 and 4.21 also show similar plots.

4.3 Part C: Diffusion Mechanism Study

4.3.1 Diffusion mechanism of tapioca chip

In this experiment, diffusion mechanism was studied at temperature of 70, 85 and 100°C in run no. C-1, C-2 and C-3 respectively. The results were plotted in semi-logarithmic paper as shown in Figure 4.22 in which the nondimensional water content (W-We/Wo-We) was plotted against time for drying. By analysis of the curves, it was concluded that:

a) In all runs straight lines are obtained which confirm that a diffusional mechanism controls the rate of drying according to eq. (2.5).

b) No constant-rate period. All drying is in the falling-rate period which has 2 stages of different diffusional mechanisms, the second stage shows slower drying rate than that of the first.

c) The decrease in water content depends on the hot air temperature. The structural changes such as shrinkage and case-hardening may concern in this pattern.

4.3.2 Diffusion coefficient of tapioca chips

The diffusion coefficient was calculated from the data taken from run no. C-4(1), C-4(2) and C-4(3). Sherwood and Newman methodswere applied and the results were comparable.

a) By Sherwood method

Sherwood equation below was used to calculate. the value of diffusion coefficient (De).

$$(\overline{W}-We)/(Wo-We) = \frac{8}{\pi^2} \cdot \frac{}{e} De\theta \, (\pi/2a)^2 \quad (eq.2.5)$$

The results from these three runs were tabulated below :

Run. No.	De, $cm^2/sec.$	Averaged value of De, $cm^2/sec.$
C - 4(1)	7.74×10^{-6}	
C - 4(2)	7.69×10^{-6}	7.63×10^{-6}
C - 4(3)	7.45×10^{-6}	

b) By Newman method

Newman [3] showed the most general situation where the surface resistance to mass transfer is not negligible compared to the resistance to internal diffusion. He extended the mathematical treatment of different geometries other than infinite slab. Figure 4.23 shows a graphical representation of his solution for infinite slab. He defined $\overline{E}$, the average fraction of evaporable water remaining in a slab of half-thickness, in terms of water content, W; ($\overline{E} = \overline{W}-We/Wo-We$). In Figure 4.23 $\overline{E}$ is shown as a function of the dimensionless term, $De\theta/a^2$ for different value of S, the mass transfer surface resistance ratio. Curve for S = 0 corresponds to Sherwood solution which referred previously. To determine the diffusion coefficient,

the drying time required for $\bar{E}$ to reach at some value must be known. The value of $De\theta/a^2$ which is associated with $\bar{E}$ is obtain from the curve in the case studied. After $De\theta/a^2$ has been obtained, De can be calculated.

The diffusion coefficient was calculated from the data from run no. C-4(1), C-4(2), and C-4(3) by this method and compared with those calculated by the cited Sherwood equation. The results were tabulated belows:

Run No.	De (Sherwood) $cm^2/sec.$	De (Newman) $cm^2/sec.$
C - 4(1)	7.74×10^{-6}	7.38×10^{-6}
C - 4(2)	7.69×10^{-6}	7.19×10^{-6}
C - 4(3)	7.45×10^{-6}	7.01×10^{-6}
Average value for C - 4	7.63×10^{-6}	7.19×10^{-6}

4.3.3 The study of the influence of temperature on the diffusion coefficient

The study was carried out under three different temperatures at 85, 70 and 55°C in run no. C-4, C-5 and C-6 respectively. De was calculated from Sherwood equation and the results are as follows:

Run No.	Temperature, °C	De, $cm^2/sec.$
C - 4	85	7.63×10^{-6}
C - 5	70	4.70×10^{-6}
C - 6	55	3.74×10^{-6}

When log De was plotted against the reciprocal of absolute temperature, $\frac{1}{T}$, a straight line resulted as shown in Figure 4.24

Table 4.1

Summary of Malaysian Size Drying Results

Run No.	Air Flowrate Kg/hr.m^2	Air Temp. °C	Bed Loading Kg.B.D.S./m^2	Drying Time min.
Variable: air flow rate				
A - 1	762	80	20.9	187
A - 2	1,144	80	20.9	166
A - 3	1,524	80	20.9	124
A - 4	2,096	80	20.9	84
Variable: hot air temperature				
A - 3	1,524	80	20.9	124
A - 8	1,524	60	20.9	196
A - 7	1,524	40	20.9	340
Variable: bed loading				
A - 4	2,096	80	20.9	84
A - 5	2,096	80	34.9	142
A - 6	2,096	80	42.9	174

(drying to W = 0.1 Kg water/Kg dry solid)

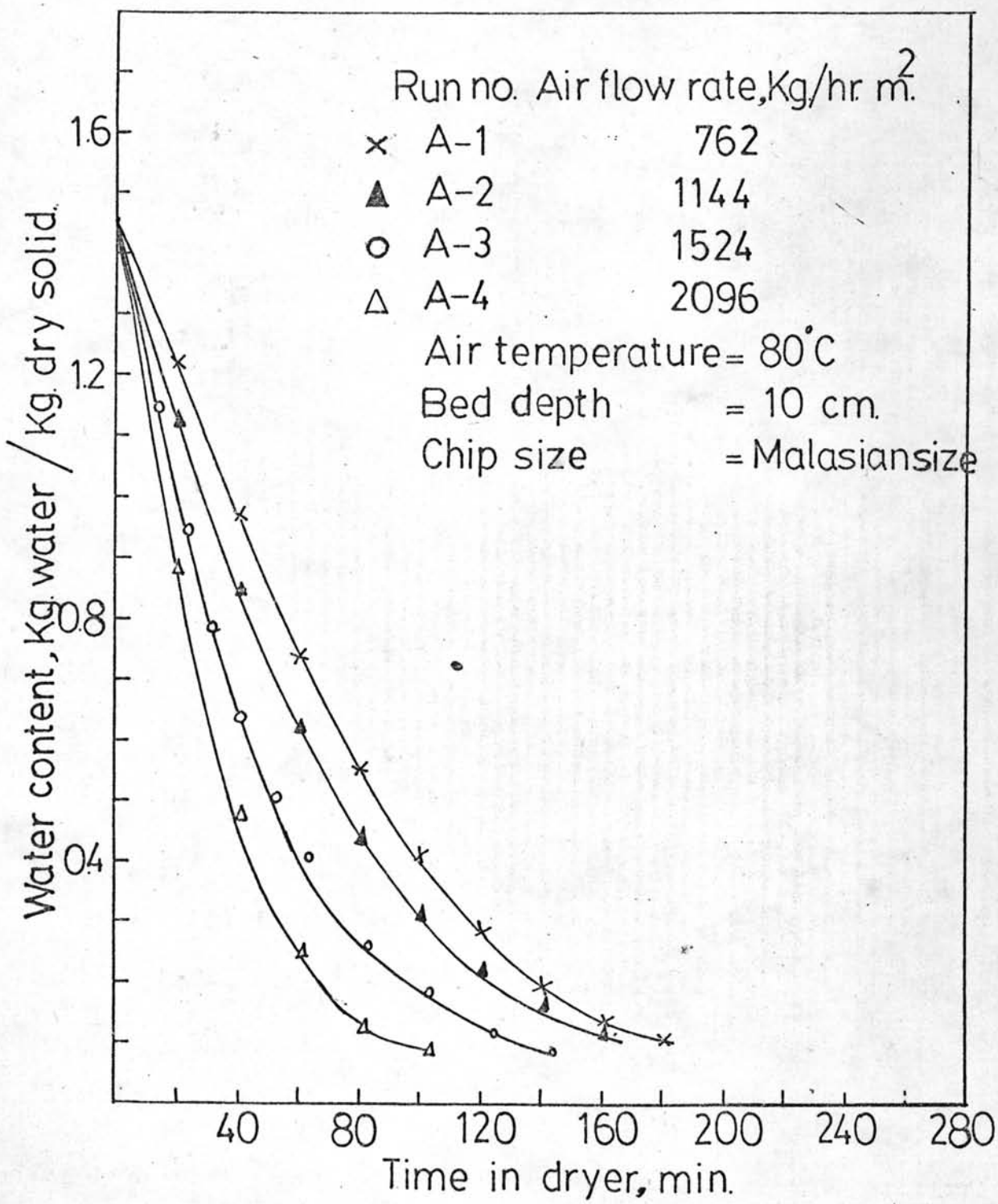

Figure 4.1 Water content V.S. drying time at various air flow rates.

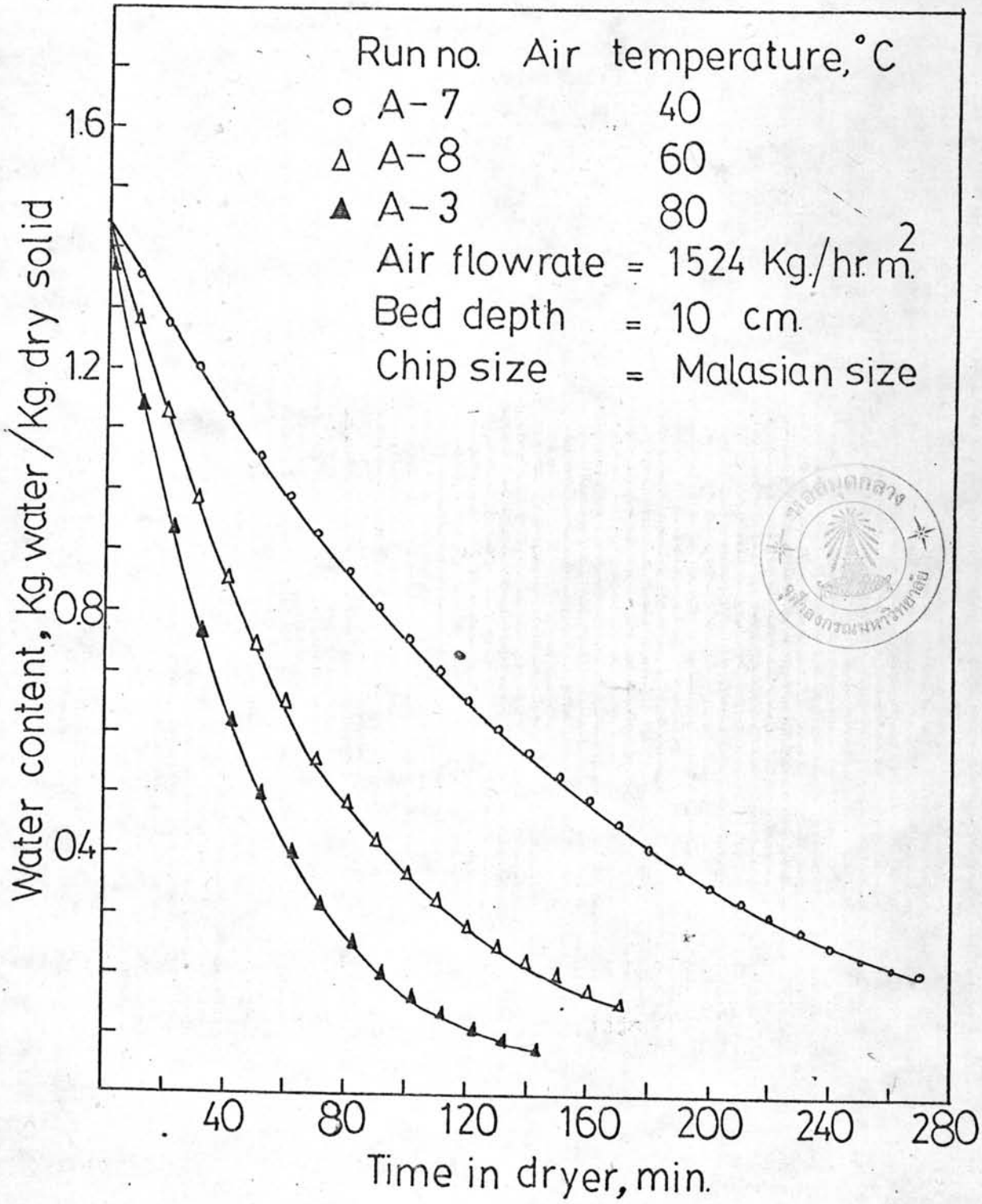

Figure 4.2 Water content V.S. drying time at various temperatures.

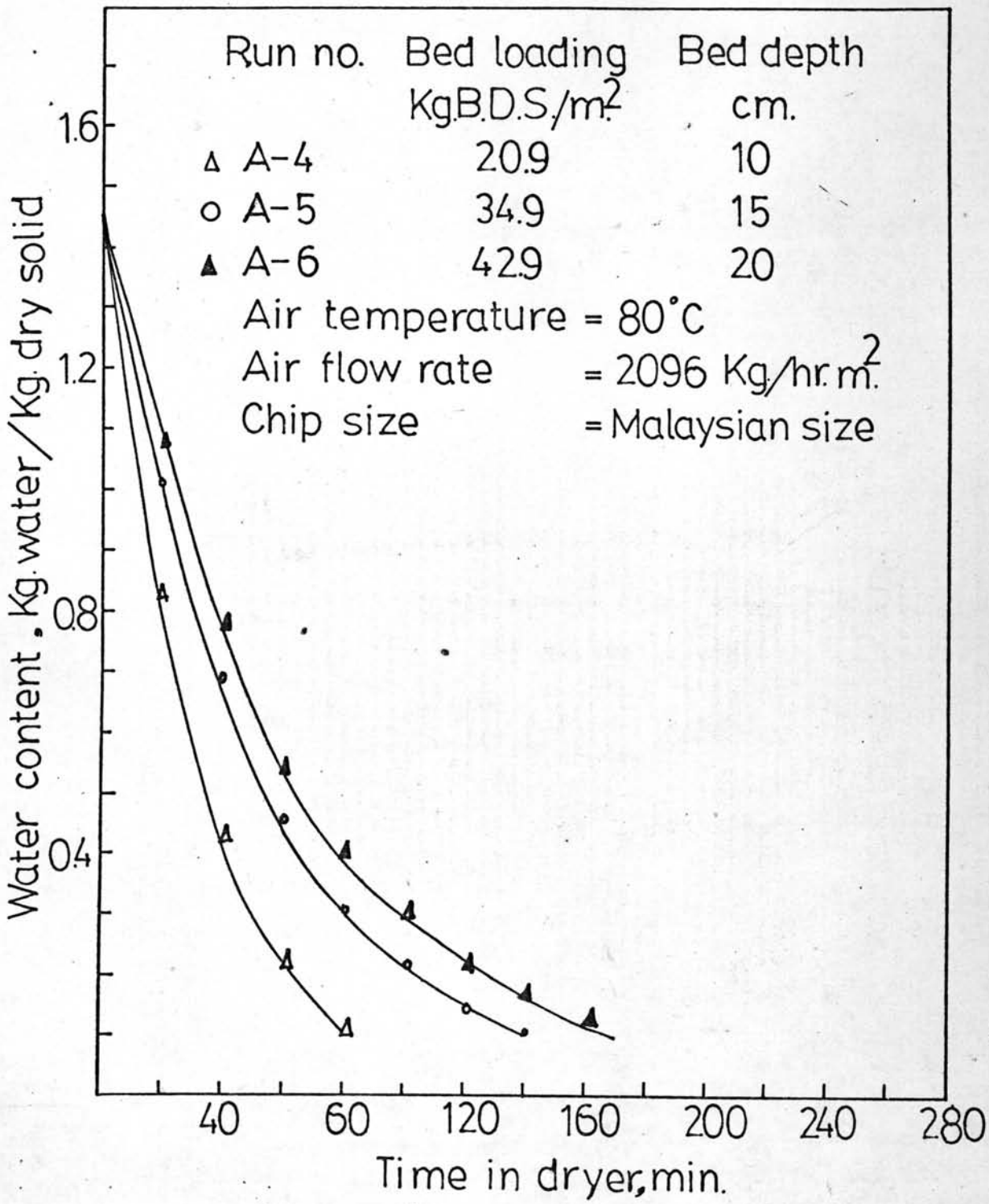

Figure 4.3 Water content V.S. drying time at various bed loadings.

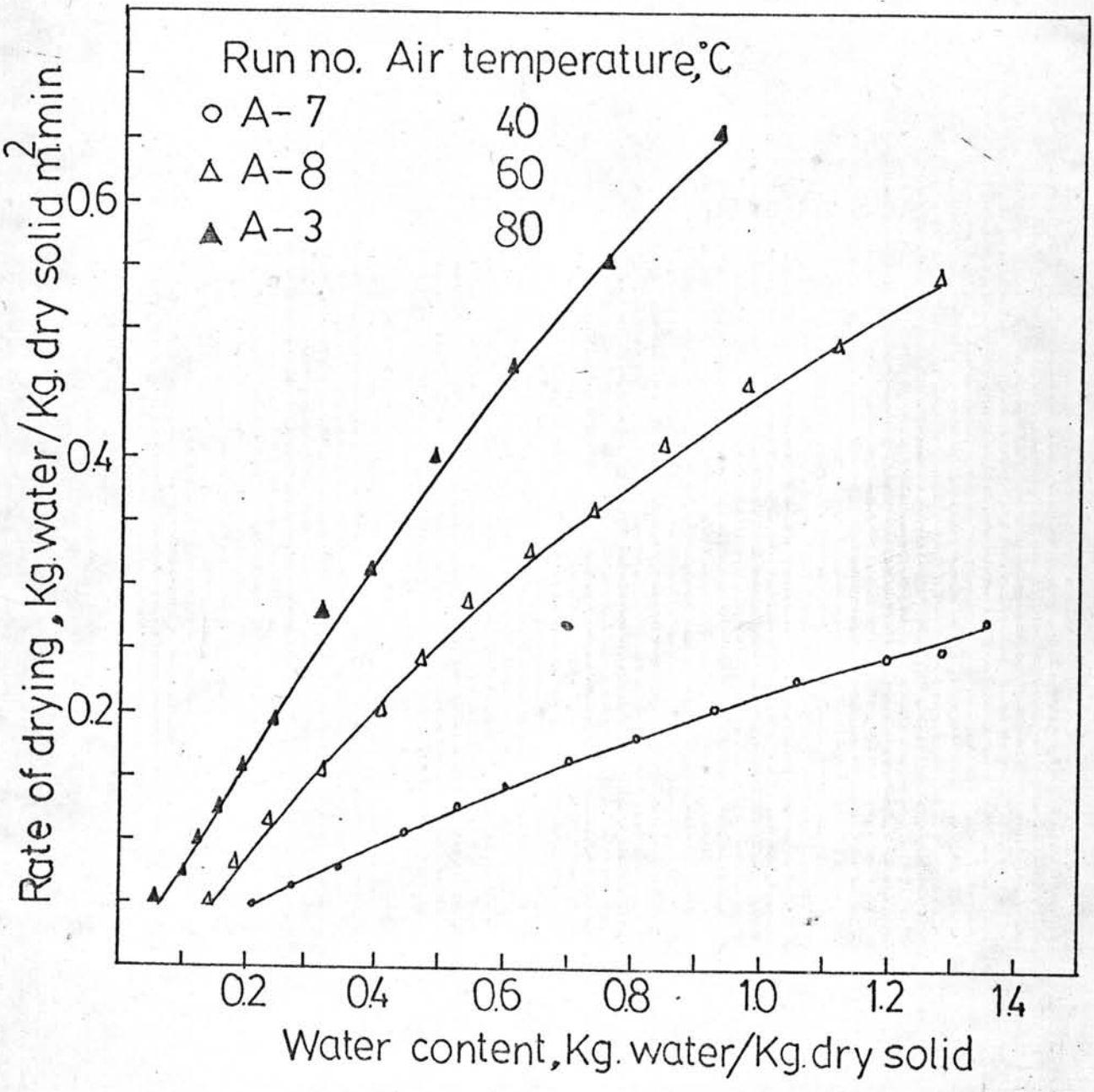

Figure 4.4 Rate of drying V.S. water content at various temperatures.

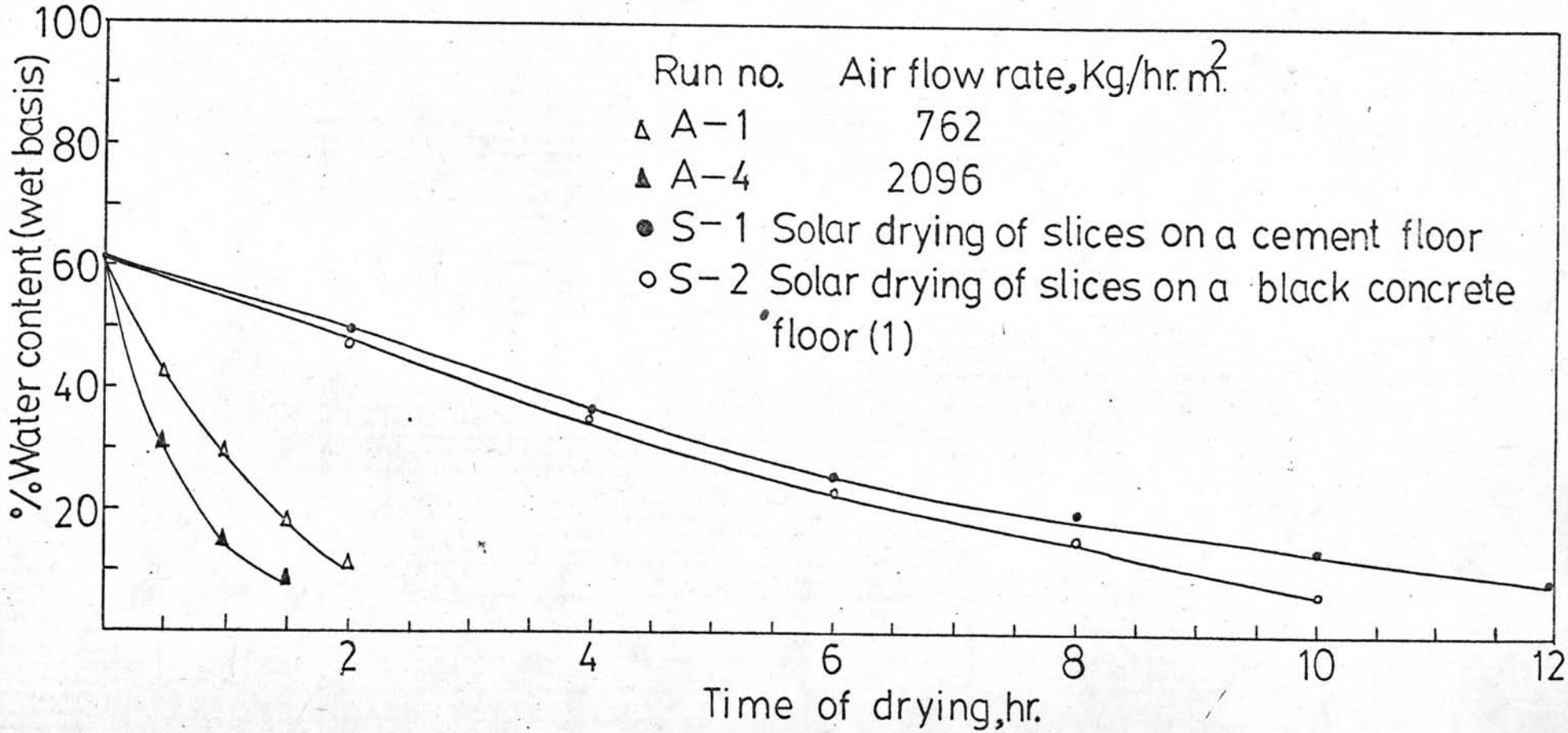

Figure 4.5 Comparison between through-circulation drying and Solar-drying by using slices from the same Malaysian blade cutter.

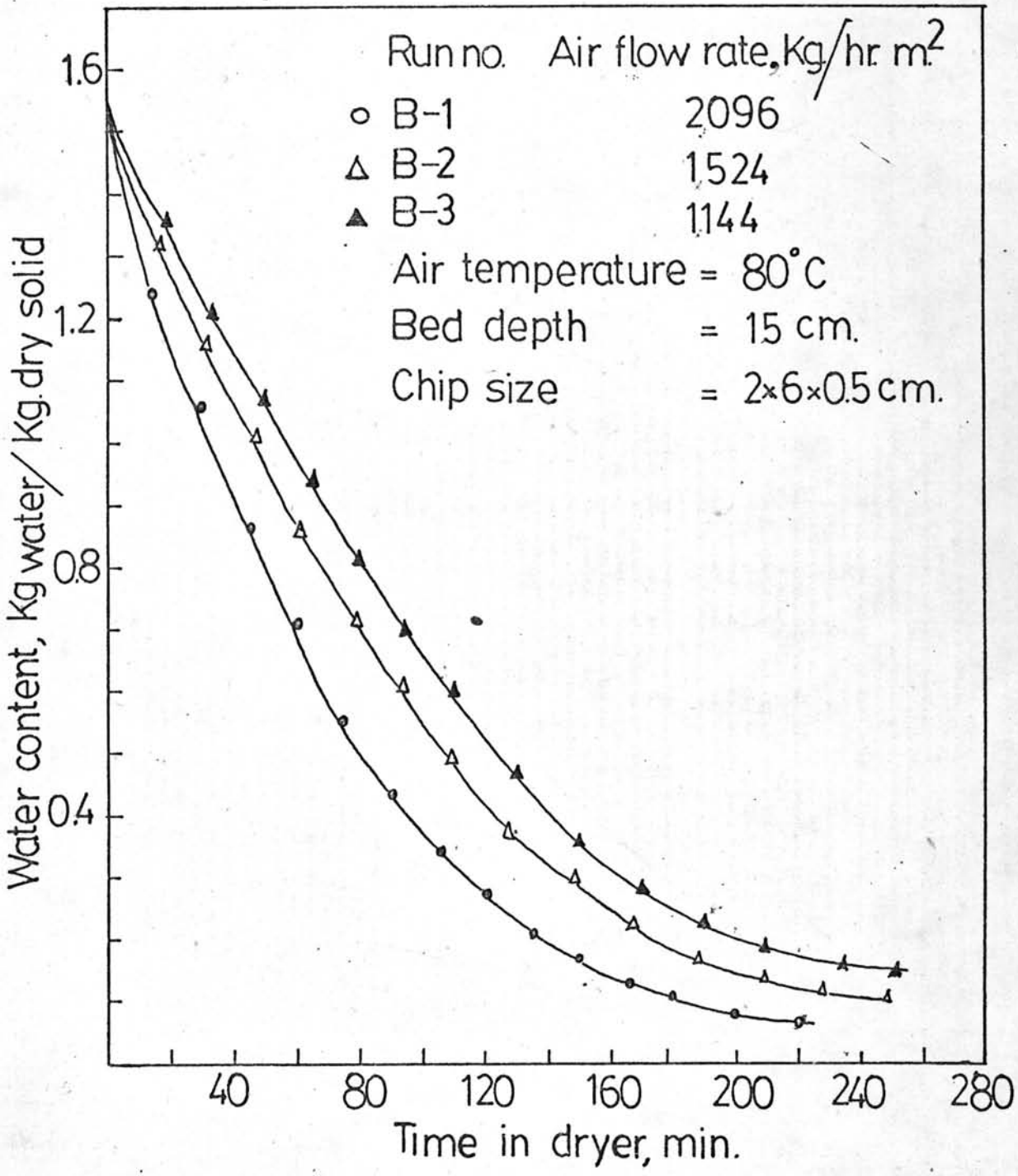

Figure 4.6 Water content V.S. drying time at various air flow rates.

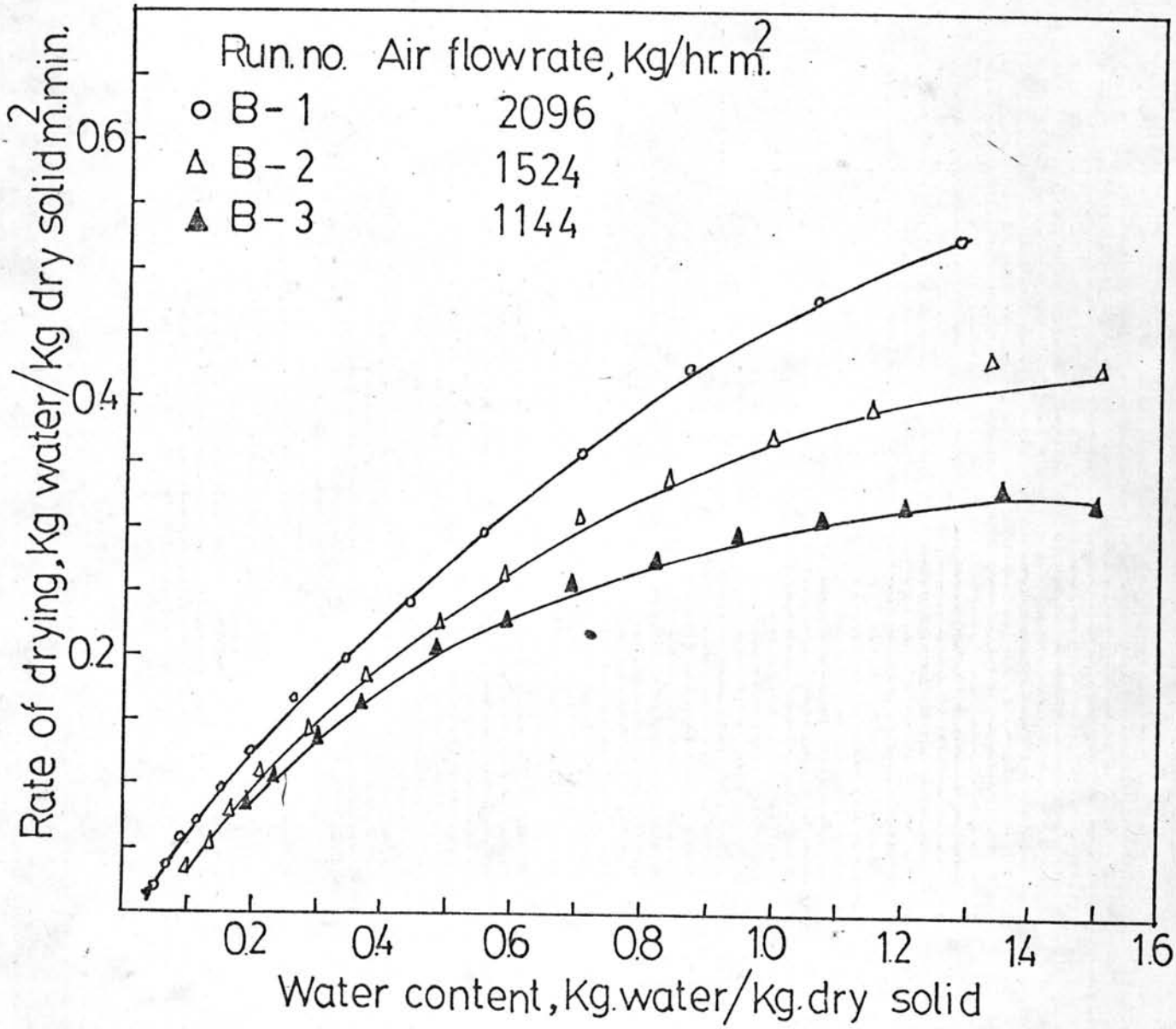

Figure 4.7 Rate of drying V.S. water content at various air flow rates.

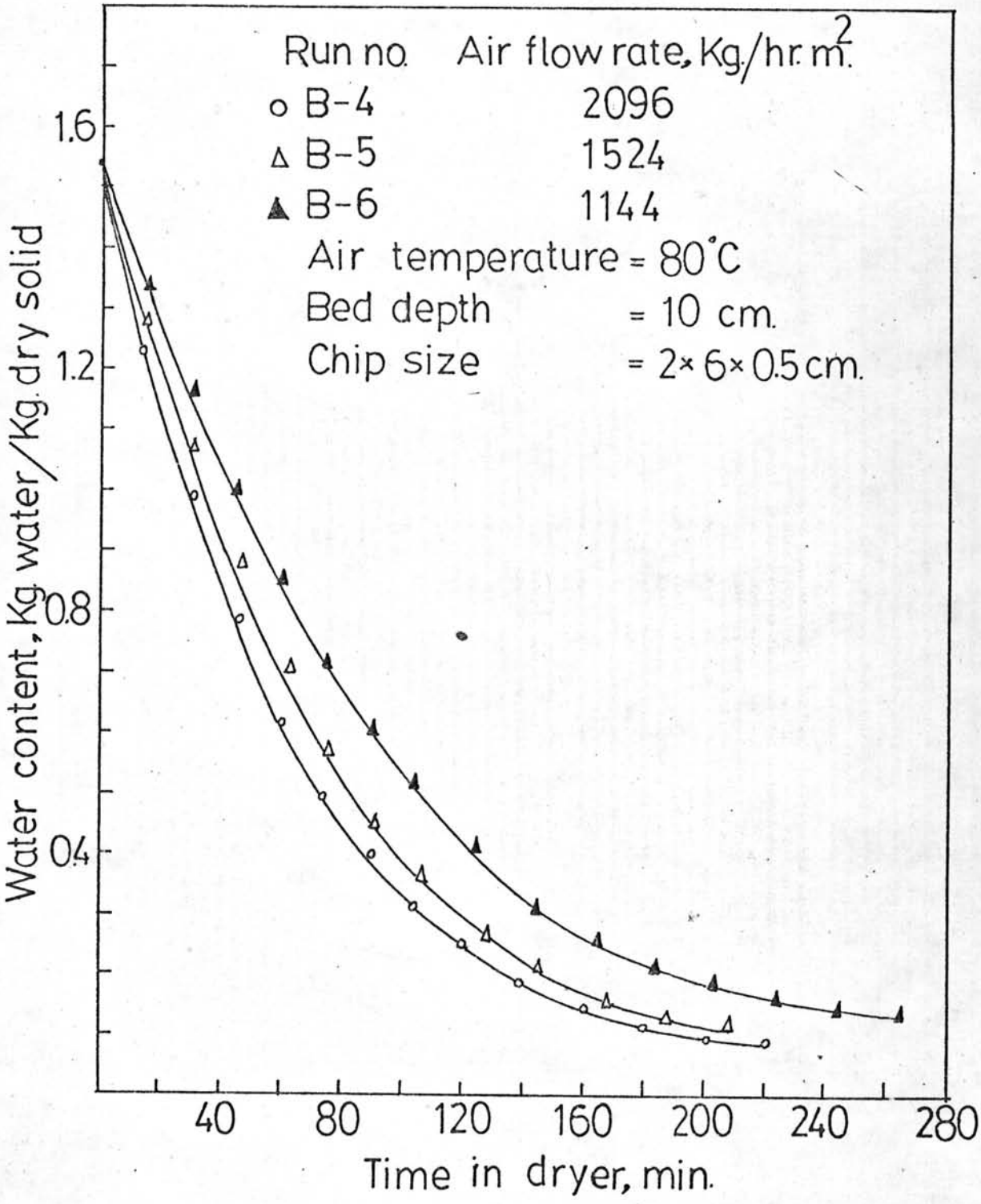

Figure 4.8 Water content V.S. drying time at various air flow rates.

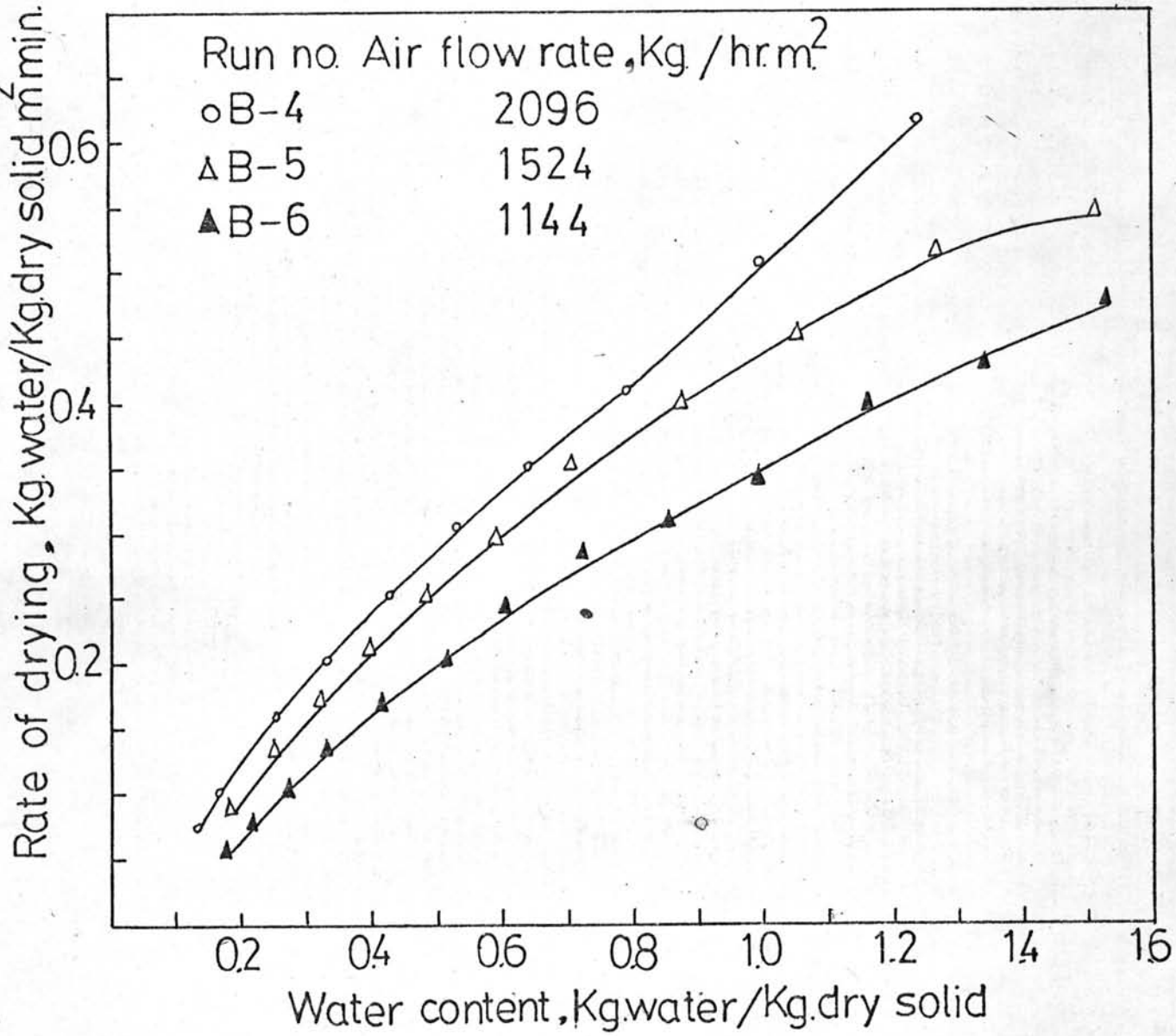

Figure 4.9 Rate of drying V.S. water content at various air flow rates.

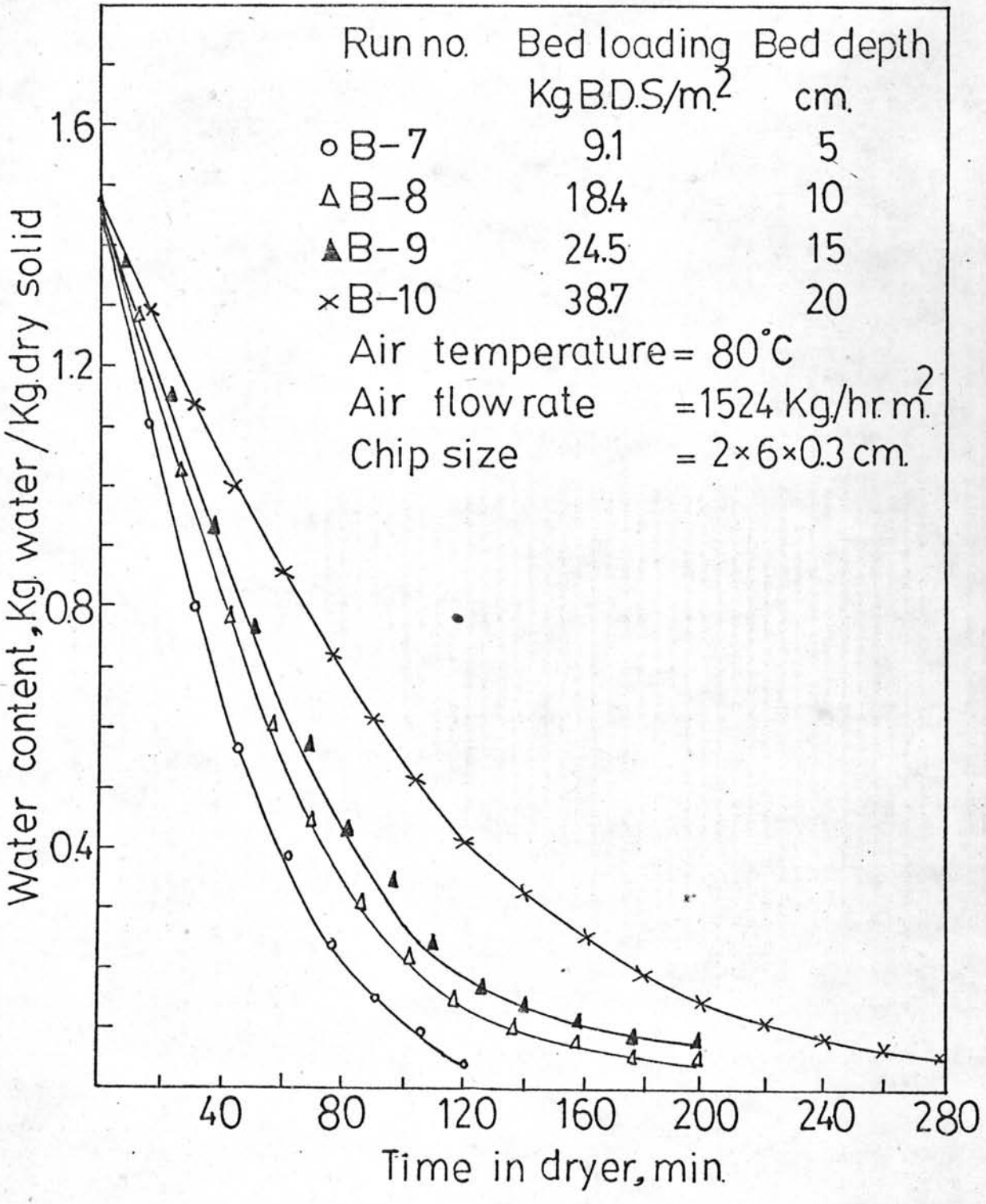

Figure 4.10 Water content V.S. drying time at various bed loadings.

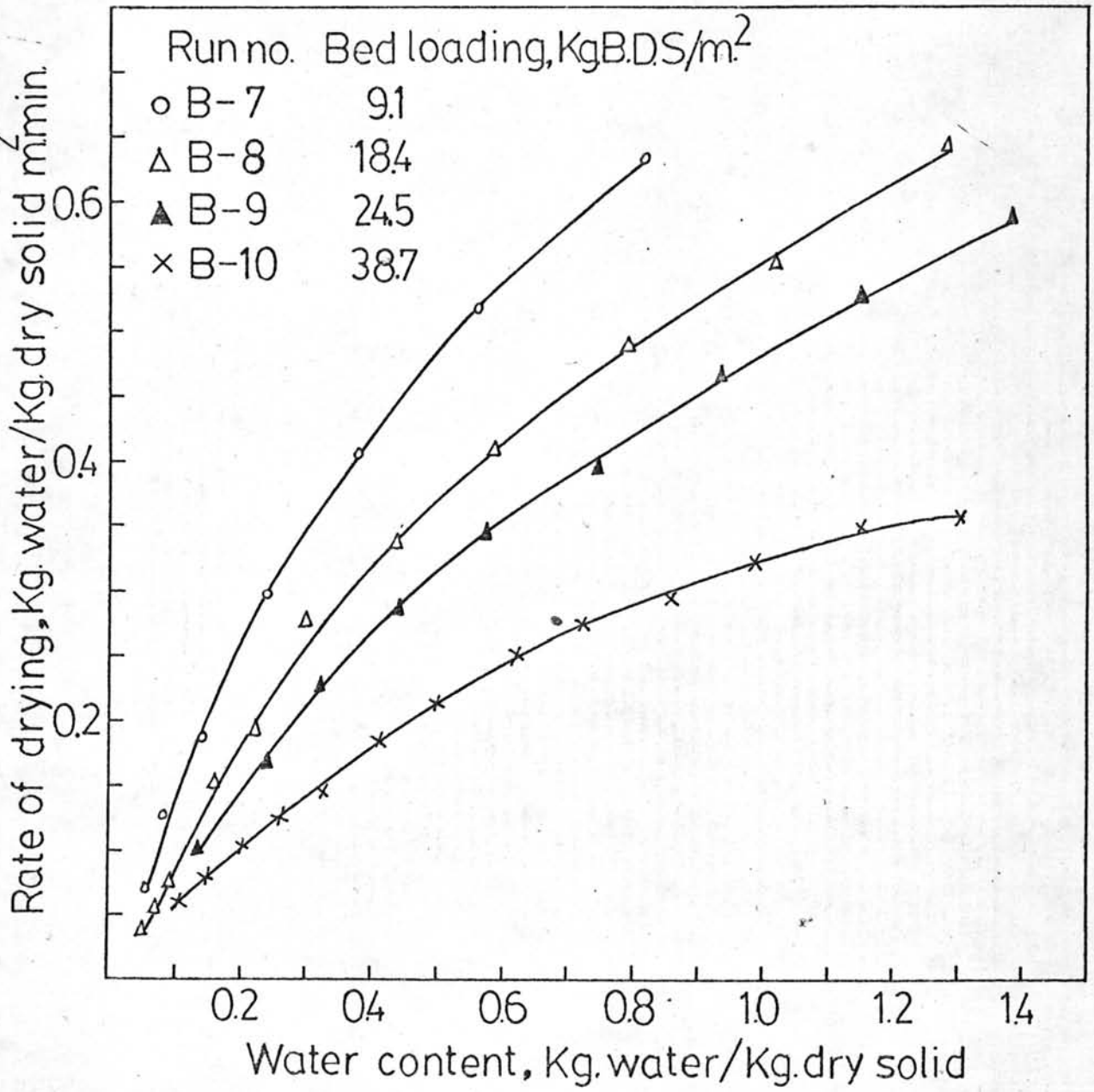

Figure 4.11 Rate of drying V.S. water content at various bed loadings.

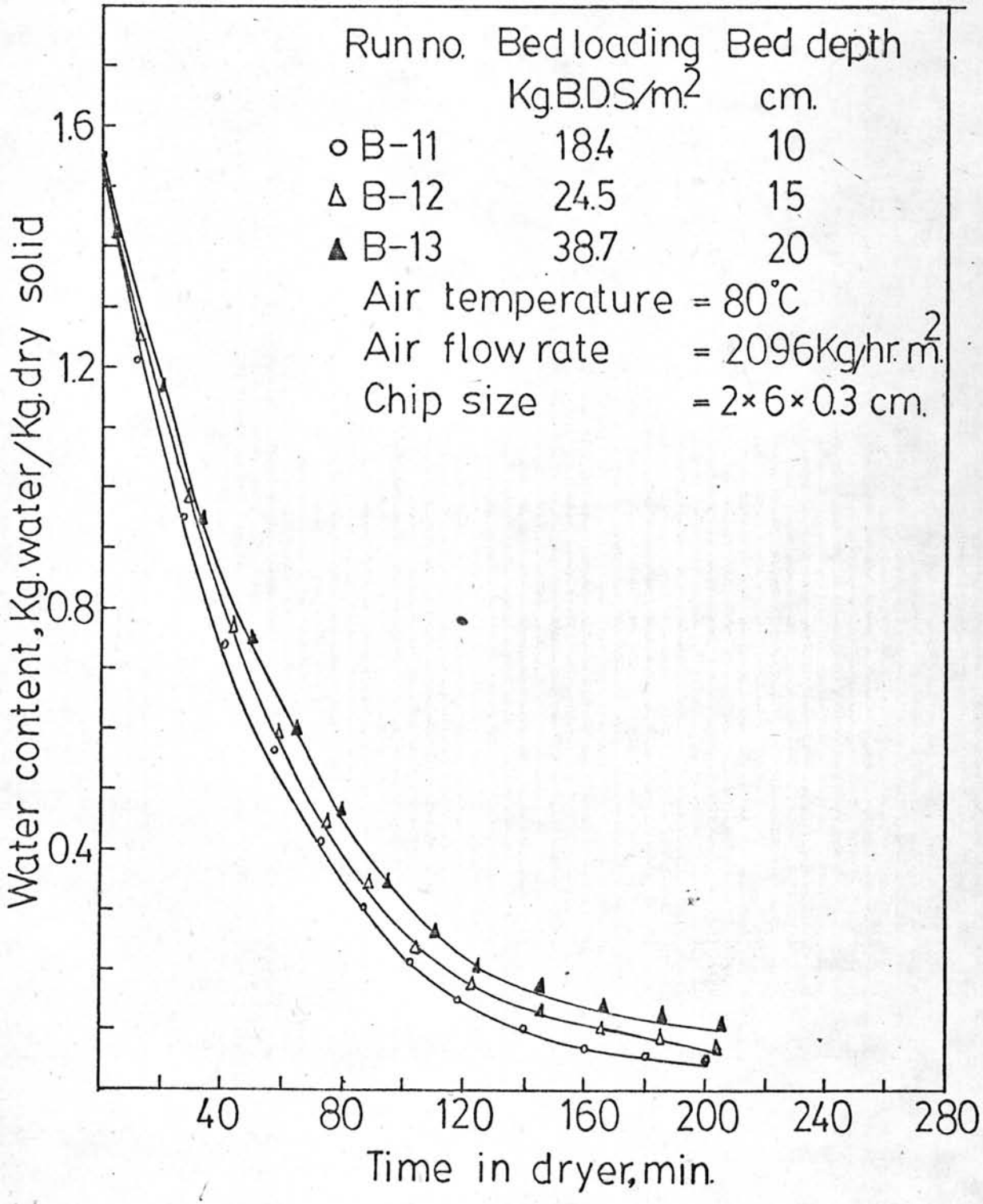

Figure 4.12 Water content V.S. drying time at various bed loadings.

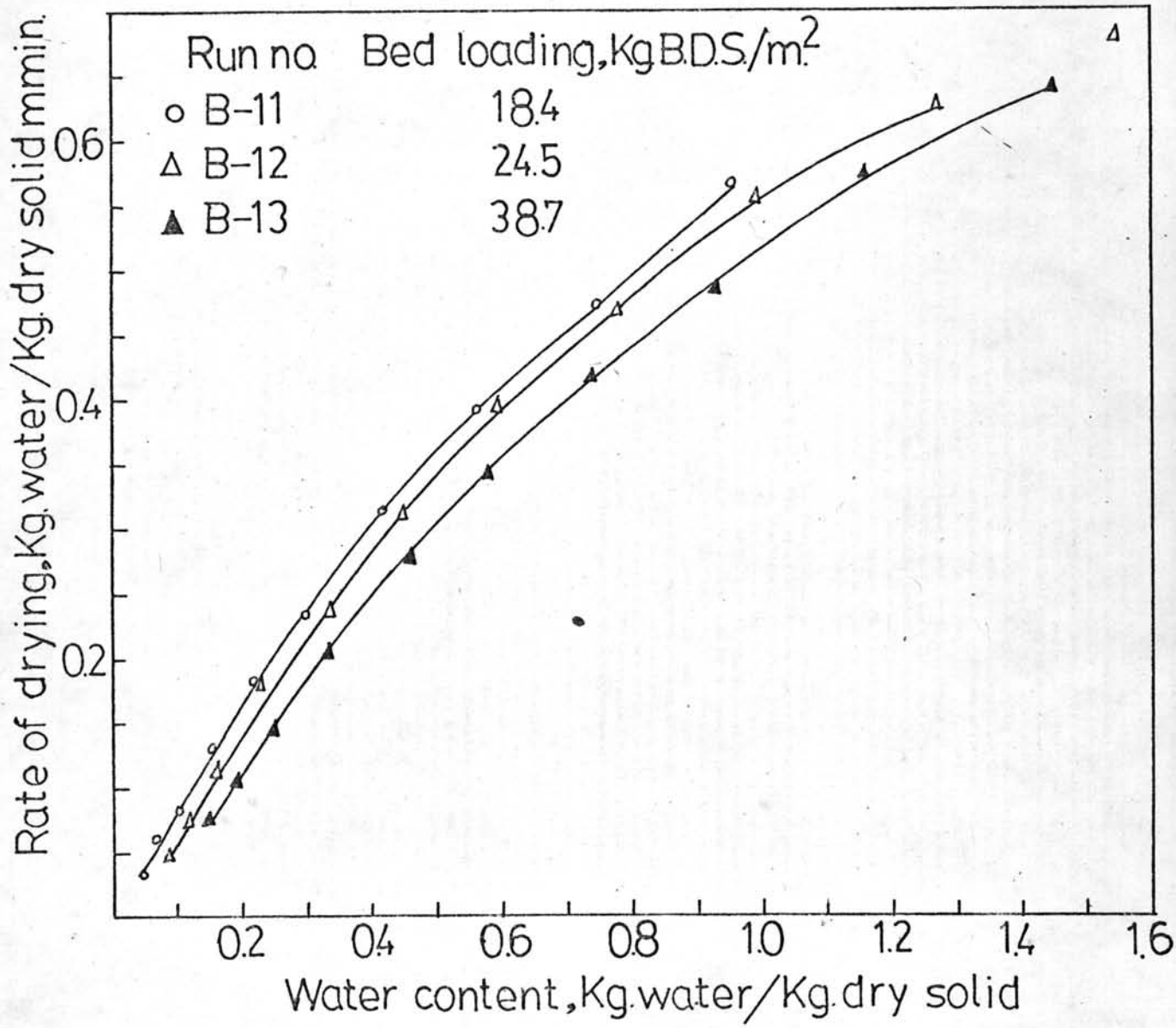

Figure 4.13 Rate of drying V.S. water content at various bed loadings.

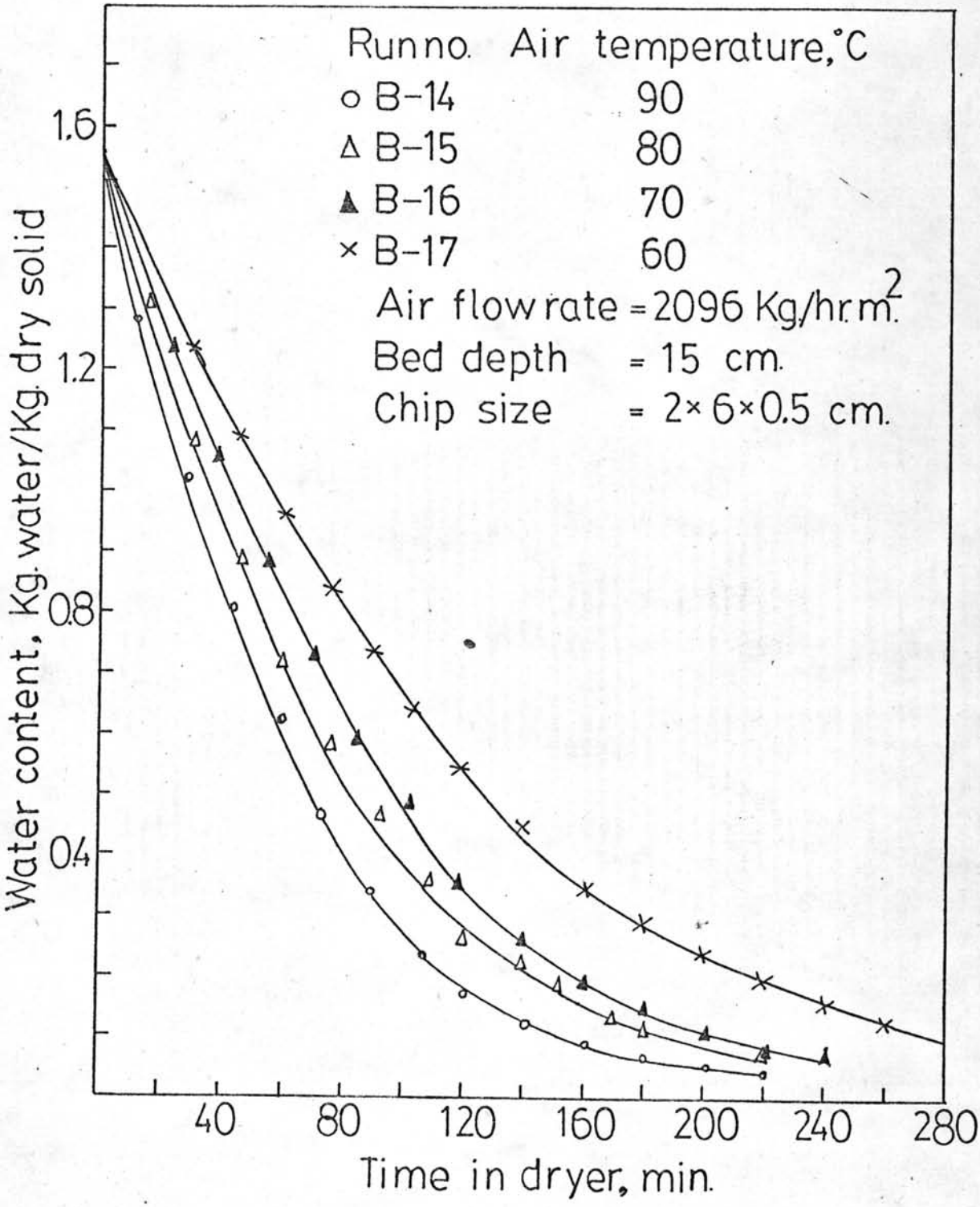

Figure 4.14 Water content V.S. drying time at various temperatures.

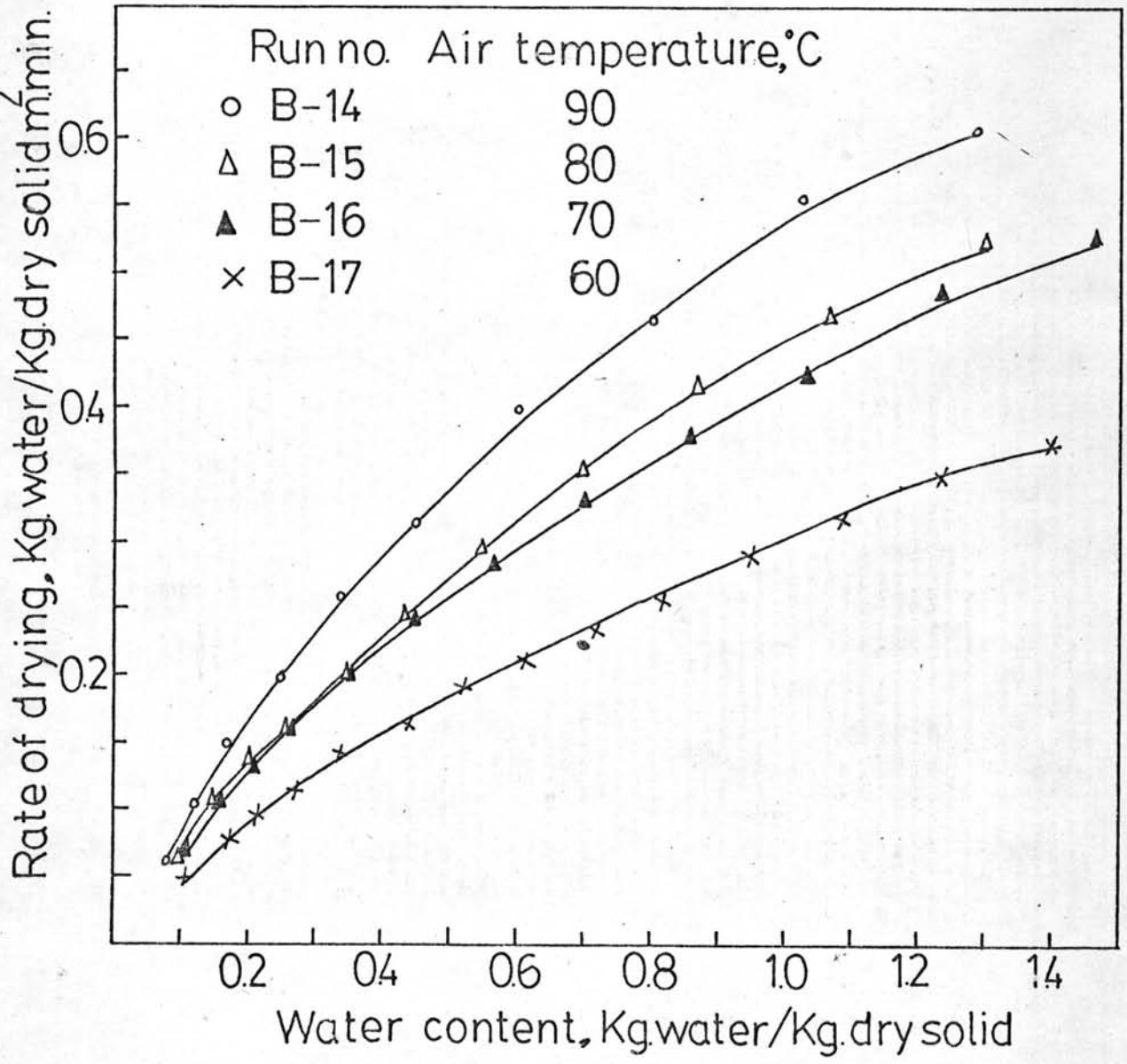

Figure 4.15 Rate of drying V.S. water content at various temperatures.

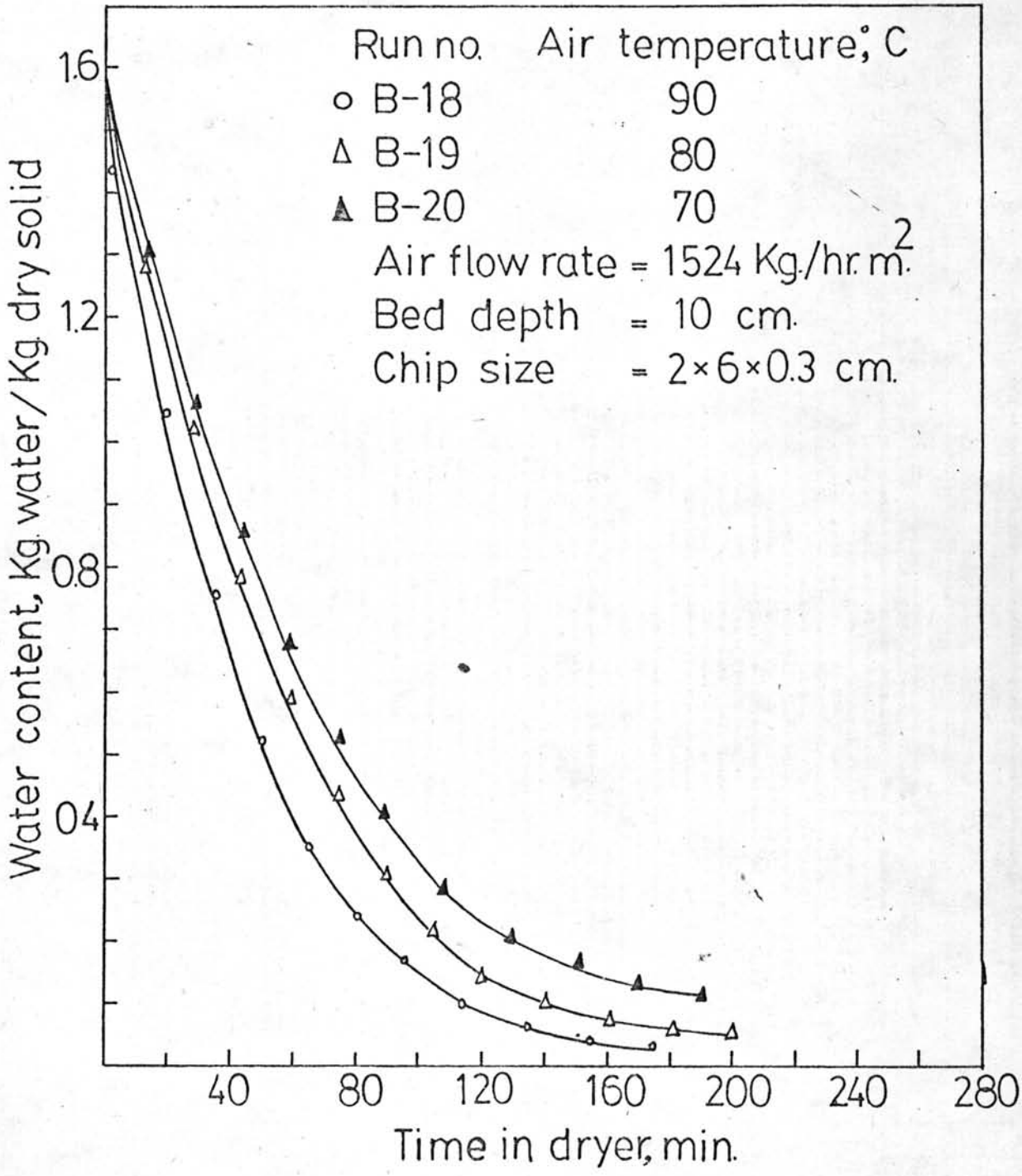

Figure 4.16 Water content V.S. drying time at various temperatures.

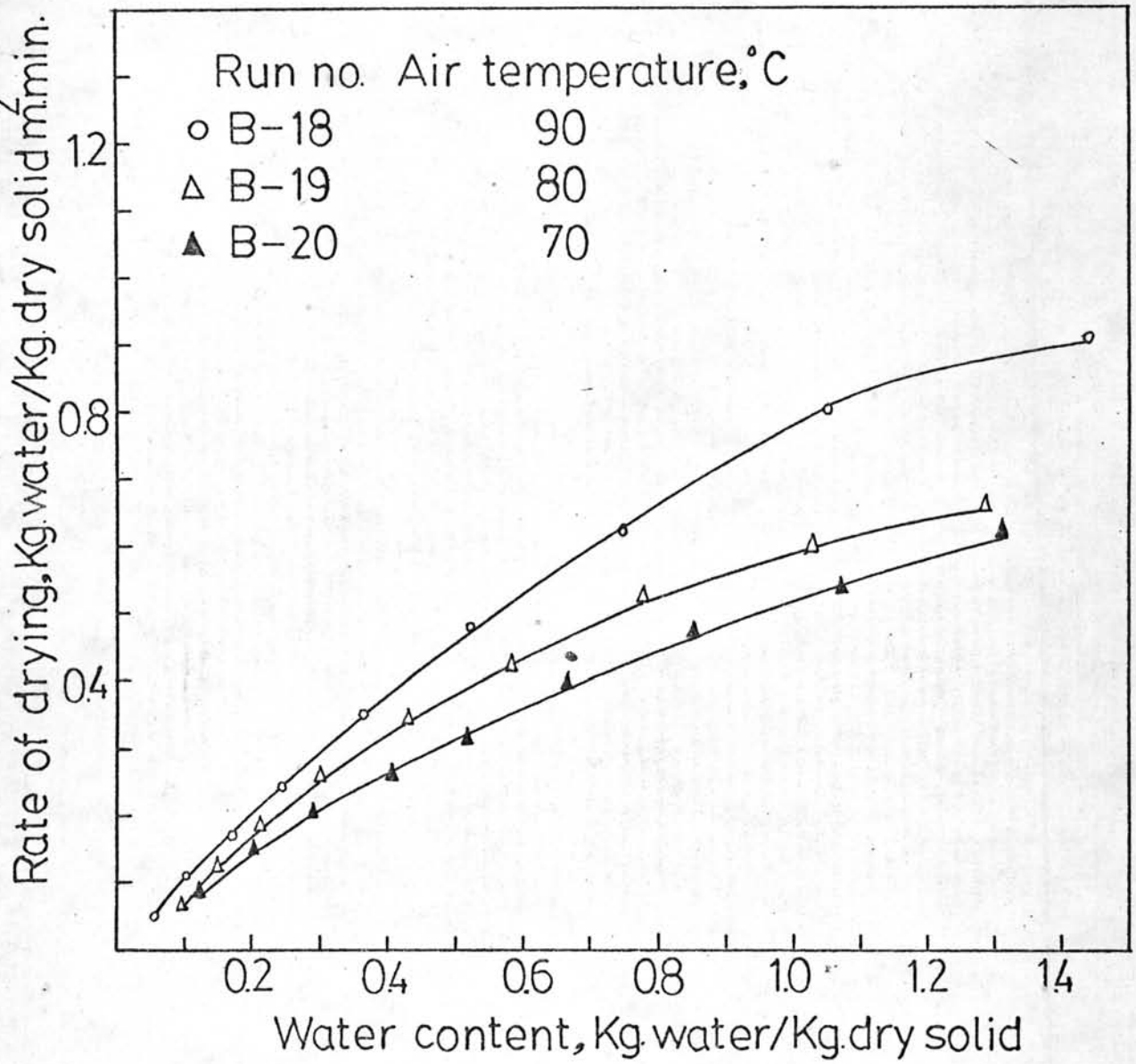

Figure 4.17 Rate of drying V.S. water content at various temperatures.

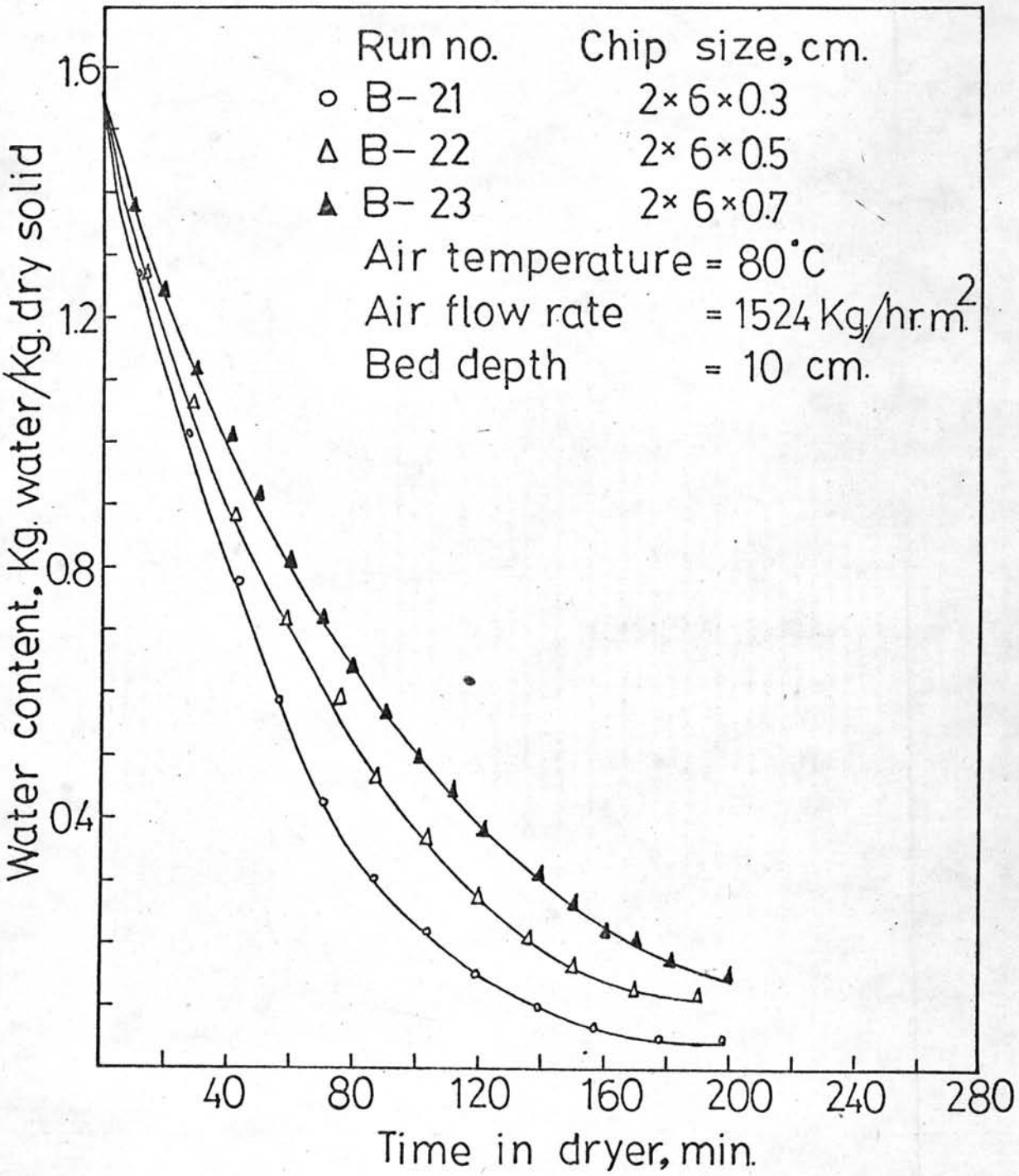

Figure 4.18 Water content V.S. drying time at various chip sizes.

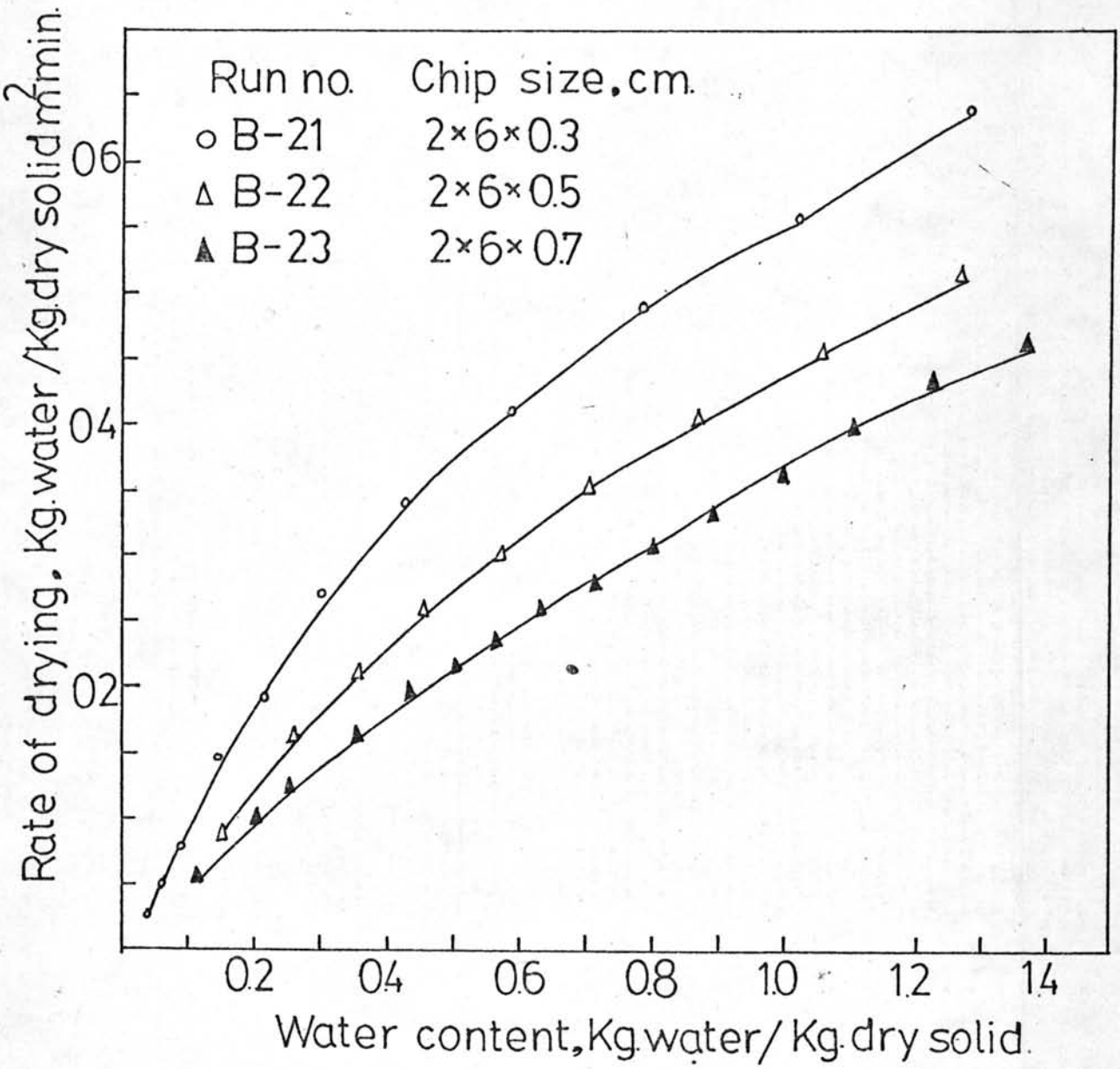

Figure 4.19 Rate of drying V.S. water content at various chip sizes.

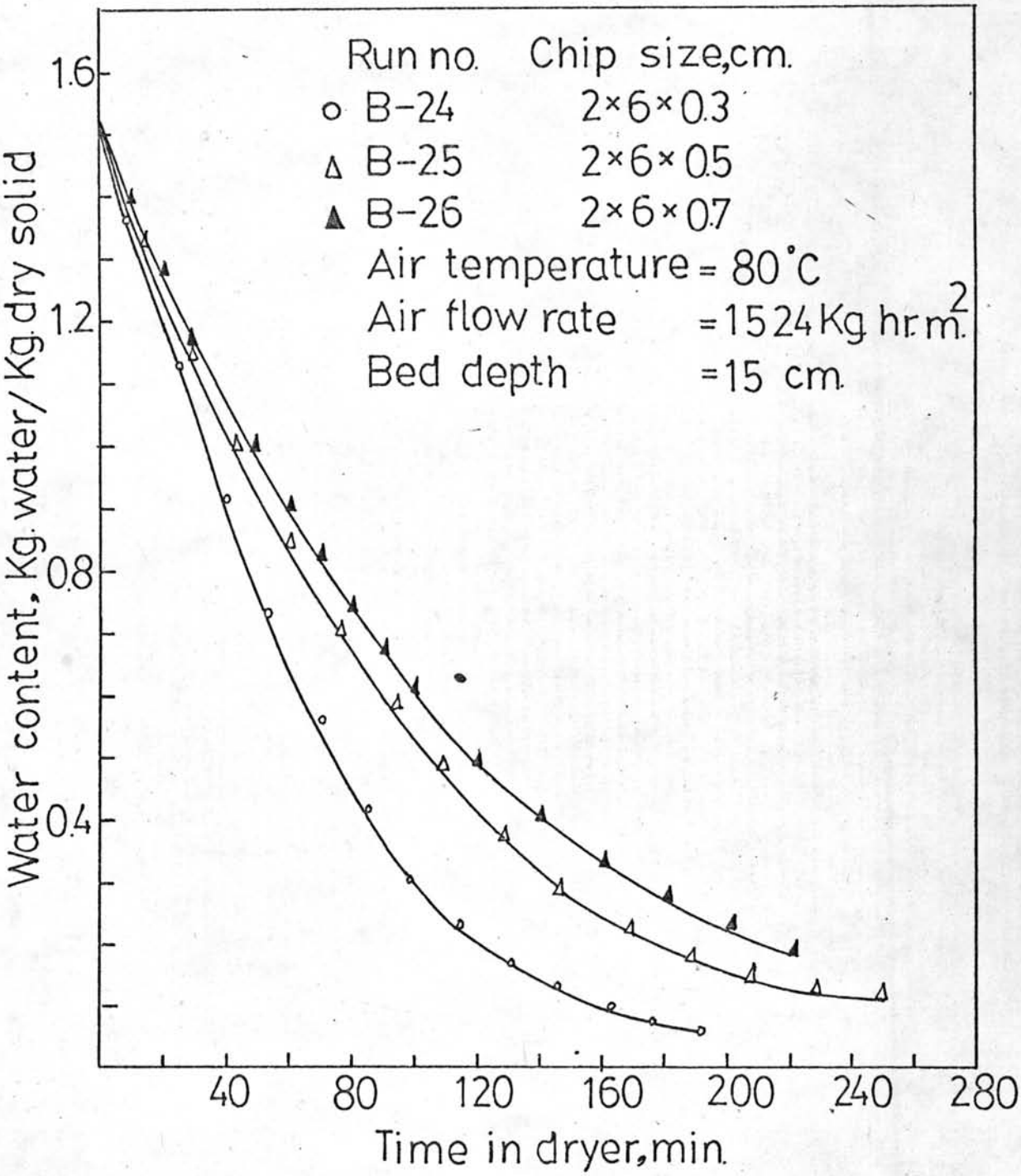

Figure 4.20 Water content V.S. drying time at various chip sizes.

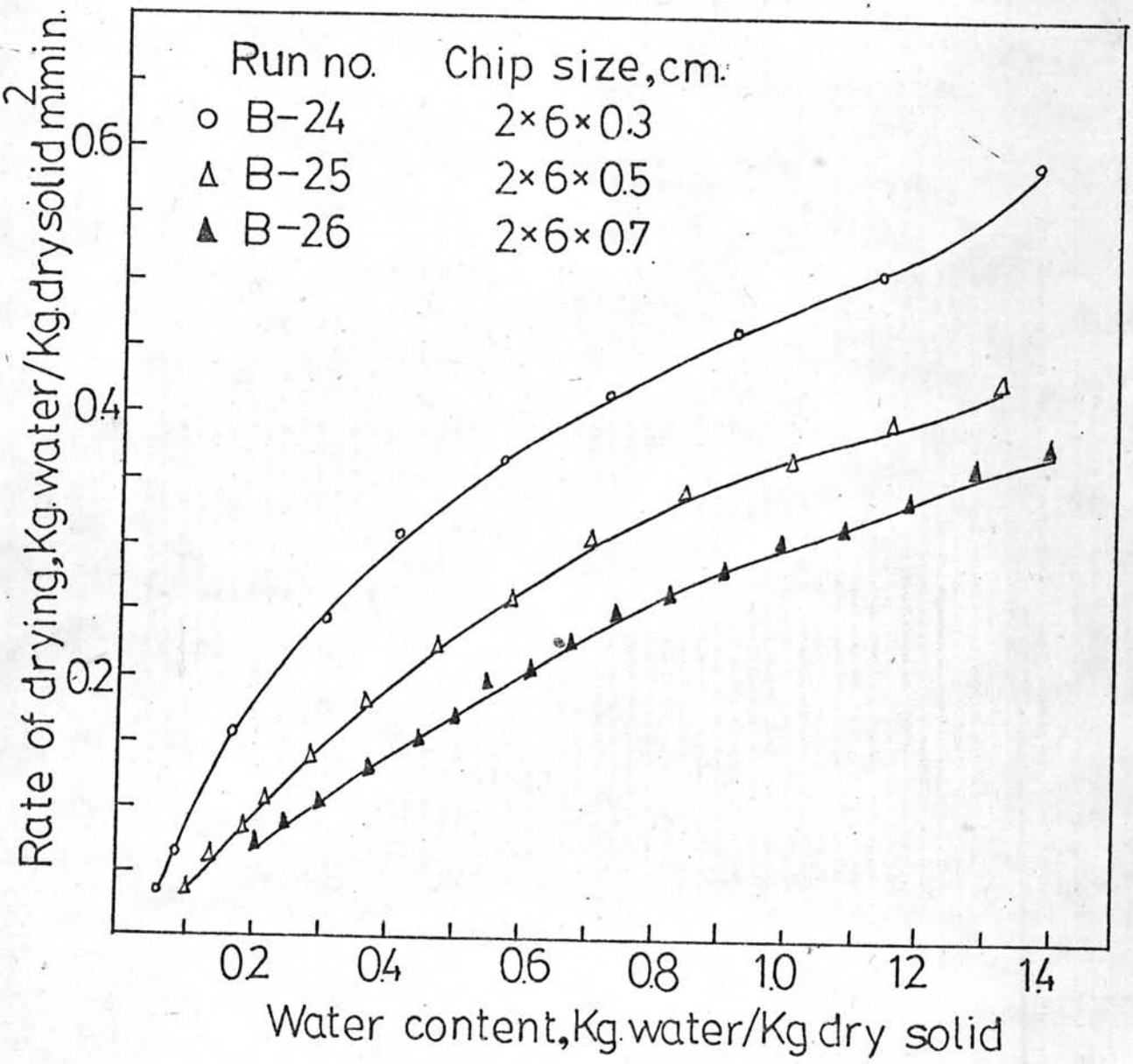

Figure 4.21 Rate of drying V.S. water content at various chip sizes.

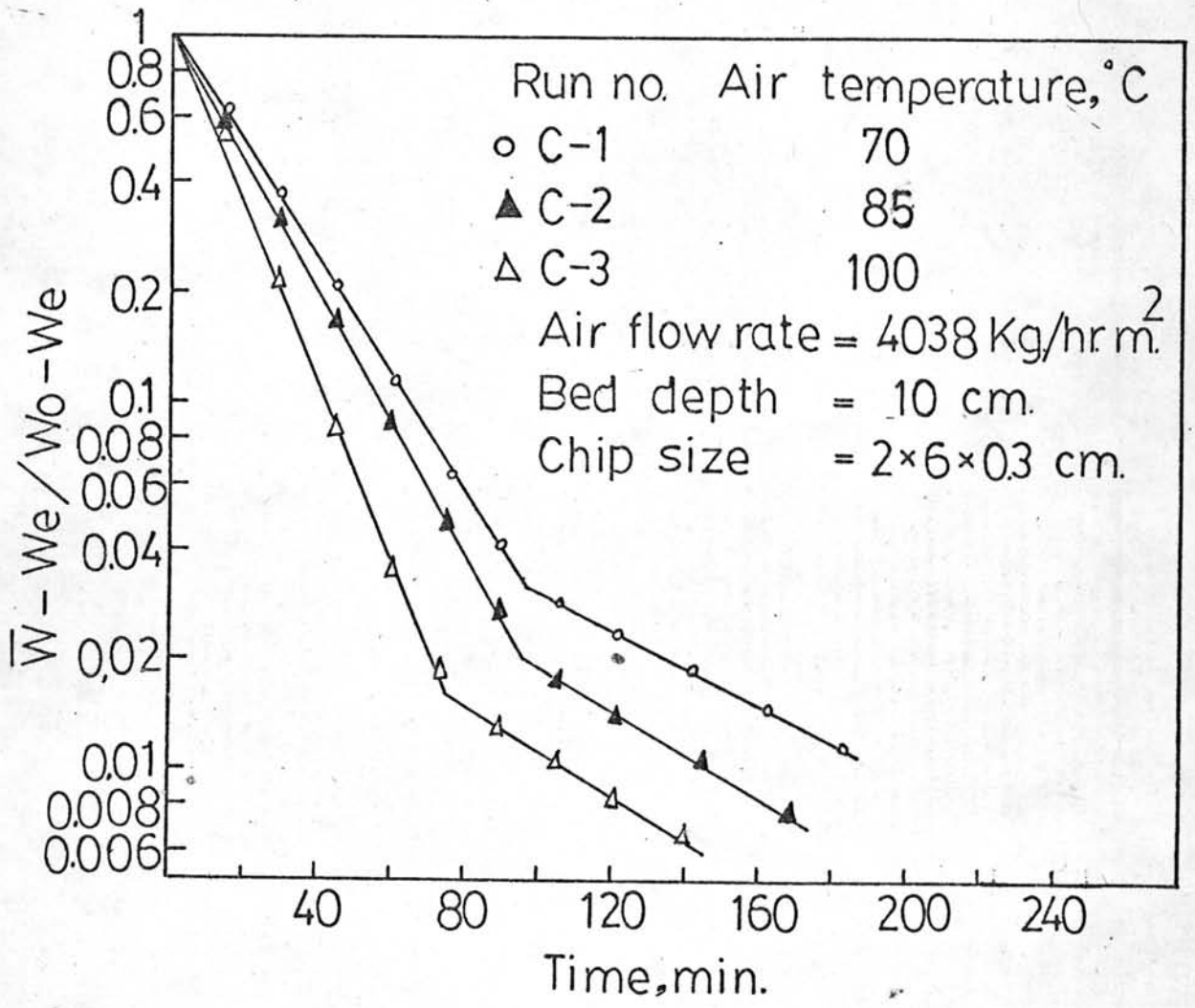

Figure 4.22 Nondimensional water content V.S. drying time.

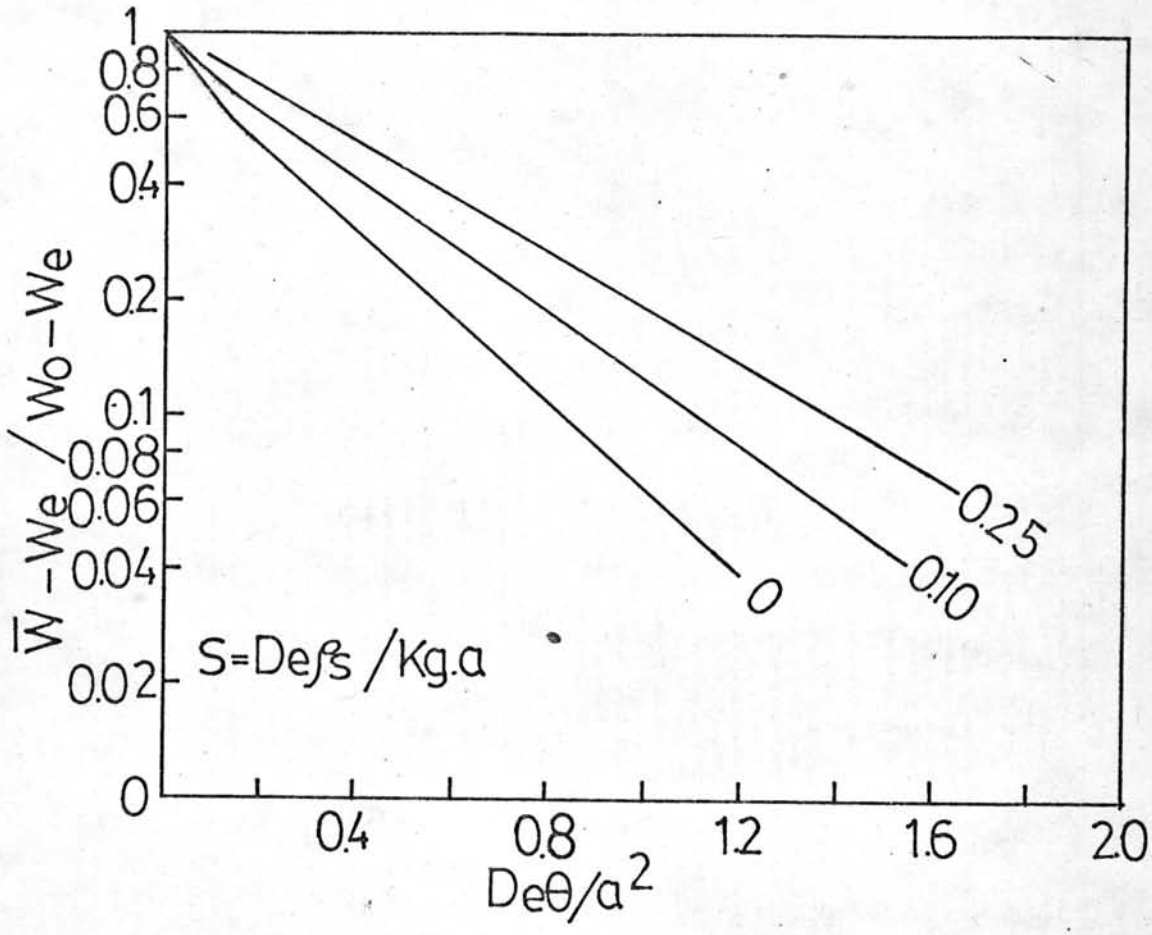

Figure 4.23 Newman method.

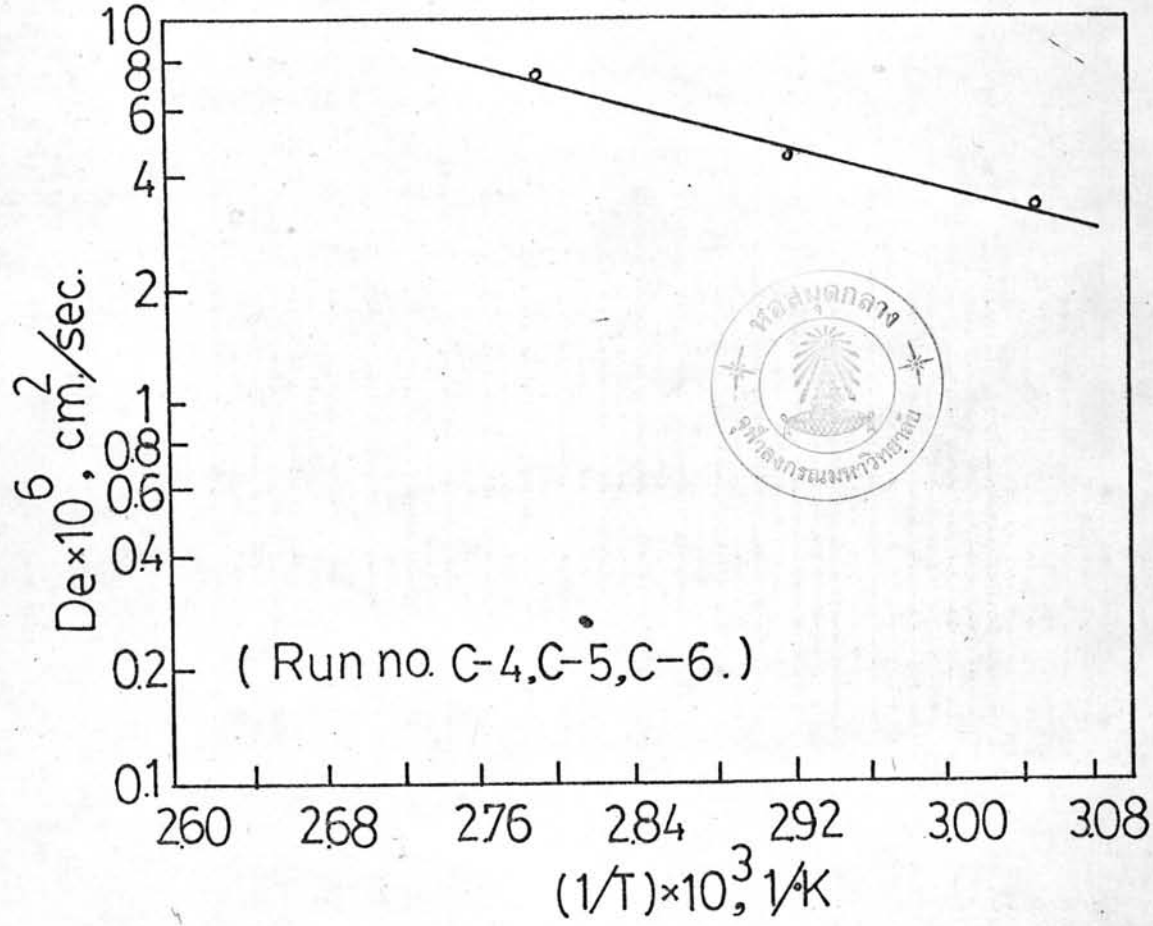

Figure 4.24 Effect of temperature on the diffusivity of moisture in tapioca.